J. Lindberg, K. Lindfors, T. Setälä, and M. Kaivola, Dipole-dipole interaction between molecules mediated by a chain of silver nanoparticles, Journal of the Optical Society of America A 24, 3427-3431 (2007).

© 2007 Optical Society of America (OSA)

Reprinted with permission.

Dipole–dipole interaction between molecules mediated by a chain of silver nanoparticles

J. Lindberg,* K. Lindfors, T. Setälä, and M. Kaivola

Department of Engineering Physics and Mathematics and Center for New Materials, Helsinki University of Technology (TKK), P.O. Box 3500, FI-02015 TKK, Finland
**Corresponding author: Jari.Lindberg@tkk.fi*

Received May 15, 2007; accepted August 11, 2007;
posted September 4, 2007 (Doc. ID 83081); published October 3, 2007

We study the dipole–dipole coupling between two fluorescent molecules in the presence of a chain of metallic nanoparticles. We analyze the spectral behavior of the coupling strength and its dependence on the molecular orientation. Our results show that for certain resonant wavelengths the coupling strength between the molecules is greatly enhanced and is strongly polarization sensitive. We also demonstrate how metallic nanoparticles can be utilized in implementing a polarization-sensitive coupler. © 2007 Optical Society of America
OCIS codes: 260.2160, 260.5740, 290.5850.

1. INTRODUCTION

The radiative properties of a molecule depend strongly on its environment. Changes in the excited-state lifetimes and radiative shifts in spontaneous emission have been extensively investigated both theoretically and experimentally [1,2]. In particular, the radiative properties of a molecule are shown to be significantly modified near metallic nanoparticles supporting plasmon resonances [3,4].

Besides altering the radiative properties of a single molecule, the environment also affects the interaction of molecules with each other, for example, in fluorescence resonant energy transfer (FRET) [1,5]. The dipole–dipole coupling between the molecules and the associated rate of energy transfer can be controlled by modifying the surroundings of the molecules. So far, the dipole–dipole coupling between two molecules or atoms has been studied in microcavities [6–8], near an optical fiber [9,10], planar dielectric surface [11], nanosphere [12], and scanning near-field optical microscope tip [13]. Furthermore, plasmon-mediated coupling through a thin metallic film has recently been demonstrated [14].

The possibility to couple emitters via plasmon resonances in metallic nano-objects offers exciting possibilities for novel plasmonic components [15,16]. For example, a chain of metallic nanoparticles has recently been utilized in transporting energy at a subwavelength scale [17–21]. Such structures are likely to find applications in transferring energy between two distant quantum systems such as molecules or quantum dots, as well as in addressing single nano-objects [22,23].

In this paper we investigate the dipole–dipole coupling between two fluorescent molecules in the presence of a chain of metallic nanoparticles. We analyze the spectral behavior of the coupling strength and its dependence on the molecular orientation in several particle configurations. We show that for certain resonant wavelengths the coupling strength between the molecules is greatly enhanced and is strongly polarization sensitive. The paper is organized as follows. In Section 2, we present the coupled-dipole method to calculate the Green tensor of the nanoparticle system, and show how the dipole–dipole coupling strength of the molecules is related to this tensor. The calculated coupling strengths are presented and discussed in Section 3. Finally, Section 4 summarizes our main conclusions.

2. THEORY

We focus on the influence of metallic nanoparticles on the FRET between two molecules. We present first how the environment-induced changes in the coupling can be accounted for by using the Green function of the system. We then describe the coupled-dipole method that we use to calculate Green's function for the nanoparticle chain configurations.

In FRET, initially one of the molecules (the donor) is in an excited state and the other (the acceptor) is in its ground state. The excitation energy is then transferred from the donor to the acceptor via a dipole–dipole coupling. We describe the molecules as three-level systems [5] with energy-level diagrams depicted in Fig. 1. The donor is excited to the state $|v_1\rangle$ by an incident optical field with angular frequency ω_1, while the acceptor is in its ground state $|g_2\rangle$. After internal relaxation, characterized by a (nonradiative) vibrational relaxation rate K, the donor resides in the excited state $|e_1\rangle$. The excited donor then couples by dipole–dipole interaction to the excited level $|v_2\rangle$ of the acceptor molecule.

The environment-induced changes on the decay rates and on the dipole–dipole coupling between the molecules are obtained from the Green tensor of the system [1,6,8]. Specifically, the dipole–dipole coupling factor J_{12} has the form [5]

$$J_{12} = -\boldsymbol{\mu}_2 \cdot \ddot{G}(\mathbf{r}_2, \mathbf{r}_1, \omega) \cdot \boldsymbol{\mu}_1, \tag{1}$$

where $\boldsymbol{\mu}_1$ and $\boldsymbol{\mu}_2$ are the transition dipole moments associated with the transitions between the levels $|e_1\rangle$ and

 © 2007 Optical Society of America

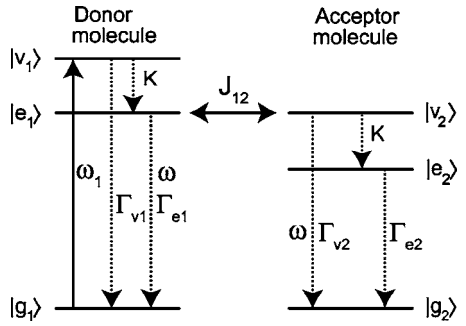

Fig. 1. Energy-level diagram of the donor and acceptor molecules. The states $|e_1\rangle$ and $|v_2\rangle$ are coupled by the dipole–dipole interaction characterized by the coupling factor J_{12}. The parameters $\Gamma_{v1,v2}$ and $\Gamma_{e1,e2}$ denote the radiative decay rates from the excited states $|v_{1,2}\rangle$ and $|e_{1,2}\rangle$ to the ground states $|g_{1,2}\rangle$, whereas K denotes the nonradiative vibrational relaxation rate. Furthermore, the energy associated with the transitions $|e_1\rangle \rightarrow |g_1\rangle$ and $|v_2\rangle \rightarrow |g_2\rangle$ is $\hbar\omega$, and ω_1 is the angular frequency of the exciting light.

$|g_1\rangle$, and $|v_2\rangle$ and $|g_2\rangle$, of the two molecules located at $\mathbf{r}_1$ and $\mathbf{r}_2$, respectively. Furthermore, $\vec{G}(\mathbf{r}_2,\mathbf{r}_1,\omega)$ is the Green tensor associated with the geometry and ω denotes the angular frequency of the light resonant with the radiative transition $|e_1\rangle \rightarrow |g_1\rangle$ (or $|v_2\rangle \rightarrow |g_2\rangle$). The coupling factor can also be written as

$$J_{12} = \hbar(\Omega_{12} - i\gamma_{12}), \tag{2}$$

where Ω_{12} is the dipole–dipole coupling strength and γ_{12} is the cooperative decay rate [5,6].

The Green tensor $\vec{G}(\mathbf{r},\mathbf{r}',\omega)$ gives at point $\mathbf{r}$ the electric field $\mathbf{E}(\mathbf{r},\omega)$, which is generated by an electric point dipole $\mathbf{p}(\mathbf{r}',\omega)$ at $\mathbf{r}'$:

$$\mathbf{E}(\mathbf{r},\omega) = \vec{G}(\mathbf{r},\mathbf{r}',\omega)\cdot\mathbf{p}(\mathbf{r}',\omega). \tag{3}$$

We consider a geometry consisting of N spherical silver nanoparticles, and approximate each particle as a point dipole, located at the center point $\mathbf{r}_n$ of the sphere, with a dipole moment $\mathbf{p}_n \equiv \mathbf{p}(\mathbf{r}_n,\omega)$, $n=1,\ldots,N$.

The electric field outside the particles can therefore be written as

$$\mathbf{E}(\mathbf{r},\omega) = \mathbf{E}_0(\mathbf{r},\omega) + \sum_{n=1}^{N} \vec{G}_0(\mathbf{r},\mathbf{r}_n,\omega)\cdot\mathbf{p}_n, \tag{4}$$

where $\vec{G}_0(\mathbf{r},\mathbf{r}',\omega)$ is the free-space Green tensor and $\mathbf{E}_0(\mathbf{r},\omega)$ is the field without the particles. The dipole moment $\mathbf{p}_n$ is proportional to the exciting field $\mathbf{E}_{exc}(\mathbf{r}_n,\omega)$, which consists of $\mathbf{E}_0(\mathbf{r}_n,\omega)$ and the fields scattered by the other particles, i.e.,

$$\mathbf{p}_n = \epsilon_0 \vec{\alpha}_n(\omega)\cdot\mathbf{E}_{exc}(\mathbf{r}_n,\omega), \tag{5}$$

where $\vec{\alpha}_n(\omega)$ is the polarizability tensor of the sphere n. Note that $\mathbf{E}_{exc}(\mathbf{r}_n,\omega)$ is not in general equal to the field that is actually present at the location of the particle, as it neglects the contribution due to the nanosphere itself [24]. However, the influence of the nanosphere on the field at its center is included in the polarizability tensor, which is taken to be that of a homogeneous and isotropic silver nanosphere. Explicitly, $\vec{\alpha}_n(\omega) = \alpha_n(\omega)\vec{U}$, where $\vec{U}$ is the unit tensor and $\alpha_n(\omega)$ is given by [4]

$$\alpha_n(\omega) = \frac{\alpha_0(\omega)}{1 - ik^3\alpha_0(\omega)/(6\pi)}, \tag{6}$$

where k is the wavenumber of the excitation field. The parameter $\alpha_0(\omega)$ in Eq. (6), known as the quasi-static polarizability, is of the form

$$\alpha_0(\omega) = 4\pi a^3 \frac{\epsilon(\omega) - 1}{\epsilon(\omega) + 2}, \tag{7}$$

with $\epsilon(\omega)$ denoting the relative permittivity of the particle material and a being the radius of the sphere. Combining Eqs. (4) and (5) we find that the unknown dipole moments are determined by the following system of coupled equations [24]:

$$\mathbf{p}_k = \epsilon_0\vec{\alpha}_k(\omega)\cdot\mathbf{E}_0(\mathbf{r}_k,\omega) + \sum_{\substack{n=1\\ n\neq k}}^{N} \epsilon_0\vec{\alpha}_k(\omega)\cdot\vec{G}_0(\mathbf{r}_k,\mathbf{r}_n,\omega)\cdot\mathbf{p}_n, \tag{8}$$

where $k=1,\ldots,N$. The above equation is solved numerically. Once the dipole moments are known, the electric field outside the particles can be calculated from Eq. (4).

The Green tensor of the nanosphere system, $\vec{G}(\mathbf{r},\mathbf{r}',\omega)$, required to calculate the coupling factor, can be obtained from Eq. (4) by evaluating the electric field $\mathbf{E}(\mathbf{r},\omega)$ when $\mathbf{E}_0(\mathbf{r},\omega)$ is the field generated by a unit point dipole at $\mathbf{r}'$. For example, the element $G_{yx}(\mathbf{r},\mathbf{r}',\omega)$ is given by the y component of the electric field, $E_y(\mathbf{r},\omega)$, when an x-oriented unit dipole is placed at $\mathbf{r}'$.

3. RESULTS

We analyze how the dipole–dipole coupling strength Ω_{12} depends on the wavelength λ corresponding to the angular frequency ω associated with the transition dipole moments $\boldsymbol{\mu}_1$ and $\boldsymbol{\mu}_2$ (see Fig. 1), and on the orientation of the interacting molecules in various nanoparticle configurations. The particles are approximated as dipoles with the polarizability of a silver sphere with radius 10 nm. For the permittivity of silver we use the data of [25]. We fix the center-to-center distance between the spheres to $d = 30$ nm. This is three times the radius of the spheres, for which distance the results obtained within the dipole model have been shown to be valid [20]. The donor and the acceptor molecules are placed at a distance of 20 nm from the nearest silver spheres. At this distance it is still reasonable to treat the silver spheres nearest to the molecules as dipoles [3,4]. For the donor and acceptor transition dipole moments we use the value 10^{-29} Cm. Our calculations do not take into account the effects of particle inhomogeneities, irregularities of the structure, or the influence of the substrate.

We consider first a straight chain of silver nanoparticles, with the acceptor and donor positioned at opposite ends of the chain. The coupling strength $|\Omega_{12}|$ for wavelengths $\lambda = 300-450$ nm is shown in Fig. 2 for different chain lengths. The transition dipole moments of the donor

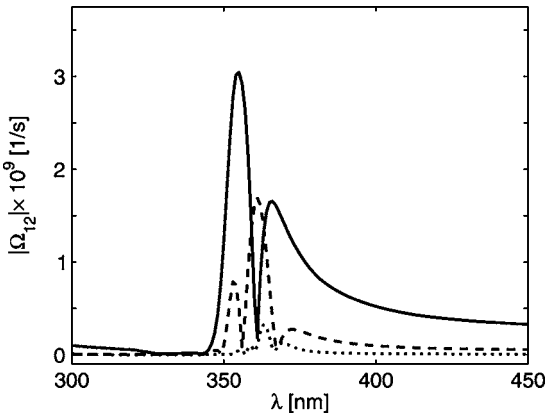

Fig. 2. The coupling strength $|\Omega_{12}|$ as a function of wavelength λ for different number of particles N in the chain. The center-to-center distance between the particles is 30 nm, and the molecules are at a distance of 20 nm from the outermost particles. Chains with $N=2$ (solid curve), 4 (dashed curve), 10 (dotted curve) particles respectively correspond to a distance of 70, 130, and 310 nm between the acceptor and the donor molecules. The dipole moments of the donor and acceptor are oriented parallel to the chain.

and acceptor molecules are both oriented parallel to the particle chain. Starting with $N=2$, we observe a strong resonance peak near $\lambda \approx 350$ nm. The main resonance peak is shifted to the red as the length of the chain increases. Compared with the free-space values, the enhancement of $|\Omega_{12}|$ at the peak is ca. 40 for $N=2$ ($\lambda=355$ nm), 200 for $N=4$ ($\lambda=361$ nm), and 150 for $N=10$ ($\lambda=363$ nm). The coupling remains relatively strong at the resonance wavelengths even for $N=10$, which corresponds to a distance of 310 nm between the acceptor and the donor. For longer wavelengths, $450\ \text{nm} < \lambda < 1000$ nm, our calculations show that the coupling strength decreases monotonically with the wavelength.

We analyze next the dependence of the coupling strength on the orientation of the molecular transition dipole moments in the straight particle chain geometry of Fig. 3(a). The donor and the acceptor molecules are again located at the opposite ends of the chain. The coupling strength $|\Omega_{12,xx}|$ and $|\Omega_{12,yy}|$, when the acceptor and the donor dipole moments are oriented parallel and perpendicular to the chain axis, are shown in Fig. 4. Due to symmetry, $|\Omega_{12,yy}|$ is equal to $|\Omega_{12,zz}|$. The coupling in the parallel orientation is observed to be considerably stronger than in the perpendicular orientation. In this particular configuration, all the terms $\Omega_{12,ij}$ ($i,j=\{x,y,z\}$ with $i \neq j$) are zero, indicating that orthogonal components do not couple. The enhancement of $|\Omega_{12,xx}|$ compared with the free-space value is approximately 220 at the resonance wavelength $\lambda=364$ nm.

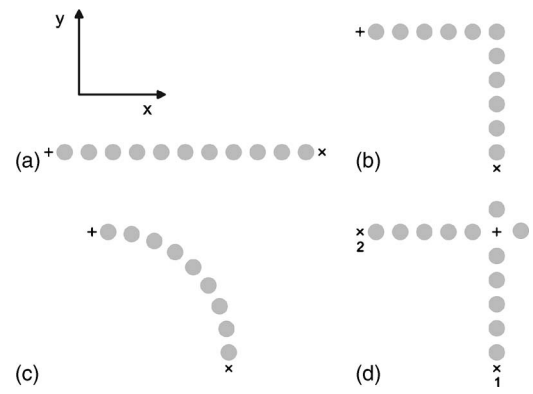

Fig. 3. Nanoparticle chain geometries: (a) straight chain, (b) right-angle corner, (c) arc (1/4 circle), and (d) coupler. The positions of the donor and acceptor are marked with (+) and (×), respectively. The center-to-center distance in (a), (b), and (d) is 30 nm, and in (c) 29.4 nm.

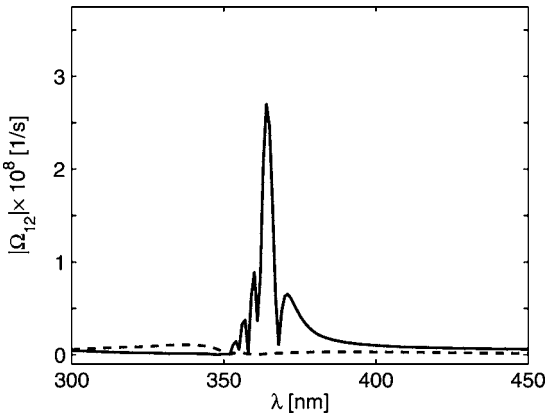

Fig. 4. Coupling strength $|\Omega_{12,xx}|$ (solid curve) and $|\Omega_{12,yy}|$ (dashed curve) as a function of the wavelength λ for the straight particle chain of Fig. 3(a).

To study the influence of curving of the particle chain, we compare the coupling strength in the geometries of Figs. 3(b) and 3(c) in which the particles form a right-angle corner and a quarter circle, respectively. The donor and the acceptor are in the same positions in both cases. In Fig. 3(b) the number of particles, particle radius, and the center-to-center distance are the same as in Fig. 3(a), i.e., $N=11$, $a=10$ nm, and $d=30$ nm. In the geometry of Fig. 3(c) the first and the last particle are in the same positions as in Fig. 3(b). However, in order to maintain the center-to-center distance as close to 30 nm as possible while keeping the sphere radius at 10 nm, the chain in Fig. 3(c) consists of only nine particles. The results are shown in Fig. 5. It is observed that the $|\Omega_{12,yx}|$ term is significantly larger than $|\Omega_{12,xx}|$ (or $|\Omega_{12,yy}|$, which is equal to $|\Omega_{12,xx}|$ due to symmetry). Despite the sharp turn in Fig.

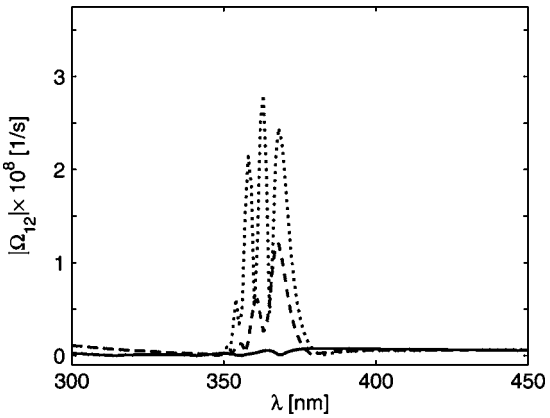

Fig. 5. Coupling strengths $|\Omega_{12,xx}|$ (solid curve) and $|\Omega_{12,yx}|$ (dashed curve) in the geometry of Fig. 3(b) (right-angle corner), and $|\Omega_{12,yx}|$ (dotted curve) in the geometry of Fig. 3(c) (arc) as a function of the wavelength λ.

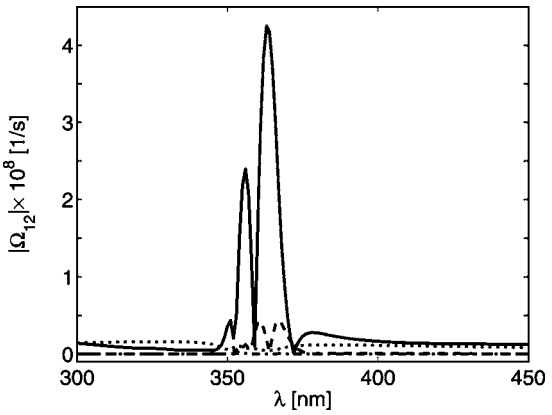

Fig. 6. Coupling strengths $|\Omega^{(1)}_{12,yy}|$ and $|\Omega^{(2)}_{12,xx}|$ (solid curve), $|\Omega^{(1)}_{12,yx}|$ and $|\Omega^{(2)}_{12,xy}|$ (dashed curve), $|\Omega^{(1)}_{12,xx}|$ and $|\Omega^{(2)}_{12,yy}|$ (dotted curve), and $|\Omega^{(1)}_{12,xy}|$ and $|\Omega^{(2)}_{12,yx}|$ (dashed–dotted curve) as a function of the wavelength λ in the geometry of Fig. 3(d).

3(b), the coupling via the chain remains strong. Compared to the free-space value the enhancement of $|\Omega_{12,yx}|$ at the peak is ca. 180 at λ=368 nm and 370 at λ=369 for the geometries of Figs. 3(b) and 3(c), respectively.

We have seen that for a straight chain the coupling is strongest when the donor and acceptor dipoles are oriented parallel to the chain (*xx* orientation). This is also the case in the curved configurations [Figs. 3(b) and 3(c)] where the strongest coupling is for the *yx* orientation. These results suggest the possible use of nanoparticle structures as orientation sensitive couplers as is discussed next.

In the geometry of Fig. 3(d), we have analyzed the coupling between the donor and two acceptors, 1 and 2, with the coupling strengths denoted by $\Omega^{(1)}_{12}$ and $\Omega^{(2)}_{12}$, respectively. The geometry consists of two straight particle chains and two additional particles that are located next to the donor to suppress the unwanted couplings $\Omega^{(1)}_{12,yx}$ and $\Omega^{(2)}_{12,xy}$. These terms would vanish for a symmetrical cross structure. The use of just two additional particles was found to provide sufficient suppression. Figure 6 shows the strength of the various couplings in the configuration. The coupling $|\Omega^{(1)}_{12}|$ to the first acceptor is dominated by the *yy* component, while the coupling $|\Omega^{(2)}_{12}|$ to the second acceptor is dominated by the *xx* component. In comparison with these, the other couplings remain weak irrespective of the donor orientation. Thus, in the geometry of Fig. 3(d), the coupling to the two ends of the chain is strongly polarization sensitive. The system acts as a polarization-sensitive coupler, where the coupling depends on the orientation of the donor dipole.

4. CONCLUSION

In this work, we have studied the dipole–dipole coupling between two molecules separated by a chain of silver nanoparticles. We obtain the coupling strength from the Green tensor of the system, which we solve using the coupled-dipole method. Our results show that at certain wavelengths the coupling strength can increase significantly compared with the free-space value. In addition, we find that the enhancement is strongly polarization sensitive. The coupling is strongest when the dipole moments of the acceptor and donor molecules are parallel to the chain. The coupling also remains relatively strong for curved particle chains. We utilized the orientation sensitivity of the coupling to demonstrate a coupler, where the coupling to different branches of the chain depends strongly on the orientation of the donor dipole. This may find applications when designing optical components for plasmonics.

ACKNOWLEDGMENTS

The authors thank the Academy of Finland for financial support (projects 116237 and 118074). J. Lindberg acknowledges a grant from the Finnish Cultural Foundation.

REFERENCES

1. R. R. Chance, A. Prock, and R. Silbey, "Molecular fluorescence and energy transfer near interfaces," in *Advances in Chemical Physics*, I. Prigogine and S. A. Rice, eds. (Wiley, 1978), Vol. 37, pp. 1–65.
2. W. L. Barnes, "Fluorescence near interfaces: the role of photonic mode density," J. Mod. Opt. **45**, 661–699 (1998).
3. P. Anger, P. Bharadwaj, and L. Novotny, "Enhancement and quenching of single-molecule fluorescence," Phys. Rev. Lett. **96**, 113002 (2006).
4. R. Carminati, J.-J. Greffet, C. Henkel, and J. M. Vigoureux, "Radiative and non-radiative decay of a single molecule close to a metallic nanoparticle," Opt. Commun. **261**, 368–375 (2006).
5. G. Colas des Francs, C. Girard, and O. J. F. Martin, "Fluorescence resonant energy transfer in the optical near field," Phys. Rev. A **67**, 053805 (2003).
6. G. S. Agarwal and S. D. Gupta, "Microcavity-induced modification of the dipole-dipole interaction," Phys. Rev. A **57**, 667–670 (1998).
7. P. Andrew and W. L. Barnes, "Förster energy transfer in an optical microcavity," Science **290**, 785–788 (2000).
8. R. L. Hartman and P. T. Leung, "Dynamical theory for modeling dipole-dipole interactions in a microcavity: the Green dyadic approach," Phys. Rev. B **64**, 193308 (2001).
9. X. M. Hua and J. I. Gersten, "Enhanced energy transfer between donor and acceptor molecules near a long wire or fiber," J. Chem. Phys. **91**, 1279–1286 (1989).
10. F. Le Kien, S. D. Gupta, K. P. Nayak, and K. Hakuta, "Nanofiber-mediated radiative transfer betweeen two distant atoms," Phys. Rev. A **72**, 063815 (2006).
11. M. Cho and R. J. Silbey, "Suppression and enhancement of van der Waals interactions," J. Chem. Phys. **104**, 8730–8741 (1996).
12. V. V. Klimov and V. S. Letokhov, "Resonance interaction between two atomic dipoles separated by the surface of a dielectric nanosphere," Phys. Rev. A **58**, 3235–3247 (1998).
13. C. Girard, O. J. F. Martin, G. Lévèque, G. Colas des Francs, and A. Dereux, "Generalized Bloch equations for optical interactions in confined geometries," Chem. Phys. Lett. **404**, 44–48 (2005).
14. P. Andrew and W. L. Barnes, "Energy transfer across a metal film mediated by surface plasmon polaritons," Science **306**, 1002–1005 (2004).
15. L. Dobrzynski, A. Akjouj, B. Djafari-Rouhani, J. O. Vasseur, M. Bouazaoui, J. P. Vilcot, H. Al Wahsh, P. Zielinski, and J. P. Vigneron, "Simple nanometric plasmon multiplexer," Phys. Rev. E **69**, 035601R (2004).
16. M. Sukharev and T. Seideman, "Phase and polarization control as a route to plasmonic nanodevices," Nano Lett. **6**, 715–719 (2006).
17. M. Quinten, A. Leitner, J. R. Krenn, and F. R. Aussenegg,

"Electromagnetic energy transport via linear chains of silver nanoparticles," Opt. Lett. **23**, 1331–1333 (1998).
18. M. L. Brongersma, J. W. Hartman, and H. A. Atwater, "Electromagnetic energy transfer and switching in nanoparticle chain arrays below the diffraction limit," Phys. Rev. B **62**, R16356–R16359 (2000).
19. S. A. Maier, P. G. Kik, H. A. Atwater, S. Meltzer, E. Harel, B. E. Koel, and A. A. G. Requicha, "Local detection of electromagnetic energy transport below the diffraction limit in metal nanoparticle plasmon waveguides," Nat. Mater. **2**, 229–232 (2003).
20. W. H. Weber and G. W. Ford, "Propagation of optical excitations by dipolar interactions in metal nanoparticle chains," Phys. Rev. B **70**, 125429 (2004).
21. C. Girard and R. Quidant, "Near-field optical transmittance of metal particle chain waveguides," Opt. Express **12**, 6141–6146 (2004).
22. G. Colas des Francs, C. Girard, J.-C. Weeber, and A. Dereux, "Near field optical adressing of single molecules in coplanar geometry: a theoretical study," J. Microsc. **202**, 307–312 (2001).
23. W. Nomura, T. Yatsui, and M. Ohtsu, "Efficient optical near-field energy transfer along an Au nanodot coupler with size-dependent resonance," Appl. Phys. B **84**, 257–259 (2006).
24. L. Novotny, B. Hecht, and D. W. Pohl, "Interference of locally excited surface plasmons," J. Appl. Phys. **81**, 1798–1806 (1997).
25. P. B. Johnson and R. W. Christy, "Optical constants of noble metals," Phys. Rev. B **6**, 4370–4379 (1972).